

Analysis of Classical Controller by Variation of Inner-loop and Controller Gain for Two-level Grid-connected Converter

Shahab Shahid Khawaja¹, Mohsin Jamil^{1*}, Qasim Awais², Umer Asgher¹ and Yasar Ayaz¹

¹Department of Robotics and Artificial Intelligence, School of Mechanical and Manufacturing Engineering, National University of Sciences and Technology, H-12 Main Campus, Islamabad, Pakistan;

mohsin@smme.nust.edu.pk

²University of Central Punjab, Lahore, Pakistan

Abstract

With the depletion of fossil fuel, the world is shifting towards the sources of alternate energy, but a major impediment in their utilization is their inter-connection with the grid. This paper builds on the model of a grid-connected converter which is used to interface the different alternate energy sources using matlab/simulink as simulation software. The classical control techniques proportional/proportional integral (P/PI) are applied on the model of the two-level grid-connected converter with LCL filter. The overall structure of the system is based upon the inner-loop capacitor current and outer-loop controller feedback. These parameters are varied and their effect is investigated in the presence of utility harmonics. The limitations and performance of the system with the variation in gain values is studied so that optimal gains can be identified.

Keywords: Grid-Connected Converters, Micro-grid, Total Harmonic Distortion

1. Introduction

A micro-grid is a collection of the Distributed Energy Resources (DER) within the main grid, which can be used in both stand-alone and grid-connected mode¹ When the DER are connected to the grid utility using a two-level converter with a LCL filter, harmonics enter the system at the Point of Common Coupling (PCC) from the grid side due to low impedance provided by the LCL filter² The harmonics are significant at the odd multiples of the fundamental frequency (50Hz) and affect the system at the resonance frequencies. Reducing the Total Harmonic Distortion (THD) of the output current is the main objective of the controller. A lot of work has been carried out in this area³⁻¹³ but still requires detailed analysis and alternative suitable controller.

There are two types of control systems (i) open-loop and (ii) closed-loop. A simple stepper motor which produces a certain torque in response to a certain voltage applied at its stator is an open-loop system. The Automatic Braking System (ABS) of a car is a closed-loop system which has a certain output feedback with which it compares the defined reference and attempts to minimize the error using a certain control action.

The limitation of conventional controllers like proportional P and proportional integral PI controllers is that they do not give good gain at the harmonic frequencies along with accurate reference tracking for a fast switching signal⁴. Our signal of interest is the grid current, which has a value of 100A (peak) and oscillates at a frequency of 50 Hz. We need a controller that has a very fast response and can suppress the harmonics at the odd

* Author for correspondence

frequencies, while simultaneously tracking the specified reference parameters⁵. In this regard, the performance of repetitive and the PR (Proportional Resonant) controllers have found to be more robust for real-time applications⁶.

2. Mathematical Modeling

We start the mathematical modeling of the three-phase two-level converter with a LCL filter at each phase. The system is complex so we start with a single-phase equivalent circuit of the two-level converter and derive its transfer function. We apply KVL to the two independent loops and KCL to the central node in Figure 1.

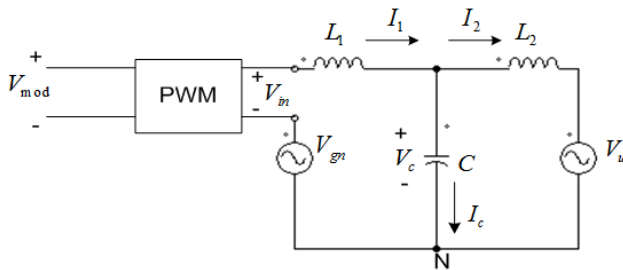


Figure 1. Single-phase equivalent of a three-phase two-level converter with LCL filter.

Here we have assumed that the ground-to-neutral voltage $V_{gn} = (V_{an} + V_{bn} + V_{cn})/3$ is equal to zero, because the capacitors are connected to the DC link. The three phase-to-neutral voltages are V_{an} , V_{bn} and V_{cn} respectively. We manipulate the KVL and KCL equations and make use of the Laplace transform⁸ to get the output current I_2 as

$$I_2(s) = \frac{V_{in}(s)}{s^3 L_1 L_2 C + s(L_1 + L_2)} - \frac{(s^2 L_1 C + 1)V_u(s)}{s^3 L_1 L_2 C + s(L_1 + L_2)} \quad (1)$$

We ignore the second part of this equation which is the disturbance injected into the system at the PCC, to derive the transfer function between the reference signal $V_{in}(s)$ and the output signal $I_2(s)$. Henceforth, the open-loop transfer function of this system is

$$G(s) = \frac{I_2(s)}{V_{in}(s)} = \frac{1}{s^3 L_1 L_2 C + s(L_1 + L_2)} \quad (2)$$

Including an inner-loop gain K_c from I_c back to the summer provides a damping term and makes the system more stable⁷.

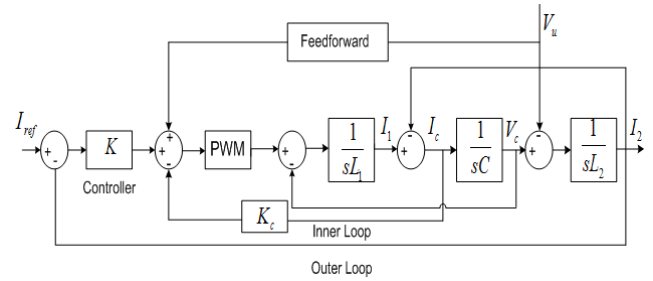


Figure 2. Modified block diagram with two-loop feedback.

The output current I_2 of the modified system Figure 2 is

$$I_2(s) = \frac{V_{in}(s)}{(L_1 L_2 C)s^3 + (K_c L_2 C)s^2 + (L_1 + L_2)} - \frac{(L_1 C s^2 + K_c C s + 1)V_u(s)}{(L_1 L_2 C)s^3 + (K_c L_2 C)s^2 + (L_1 + L_2)} \quad (3)$$

$G_1(s)$, which is the closed-loop transfer function of the two-level converter with LCL filter including the capacitive feedback damping is as (4)

$$G_1(s) = \frac{1}{(L_1 L_2 C)s^3 + (K_c L_2 C)s^2 + (L_1 + L_2)s} \quad (4)$$

The utility disturbance is defined as (5)

$$D(s) = V_u (L_1 C s^2 + K_c C s + 1) \quad (5)$$

3. Matlab Simulations

The model used for simulation is shown in Figure 3, which is a linear approximation of the single-phase equivalent of the two-level grid-connected converter.

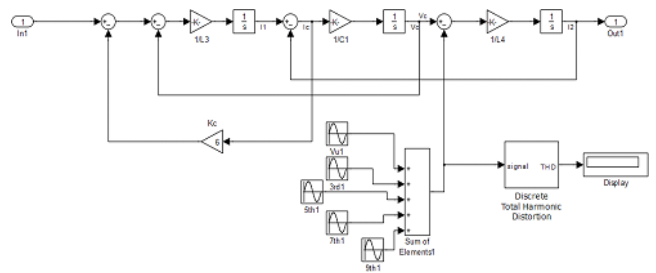


Figure 3. Simulink model of Two-Level Grid-Connected Converter.

The values of the components of the LCL filter are $L_1=350\mu\text{H}$, $L_2=50\mu\text{H}$ and $C=22.5\mu\text{F}$ ⁸. Substituting these values into (2), we find the poles of the transfer function which lie at 0 and $\pm 3.1783i$ respectively. A system with a

pole at zero is a critically stable system. From Figure 4, it is clear that the system is critically stable and will become unstable when any input signal is given to it.

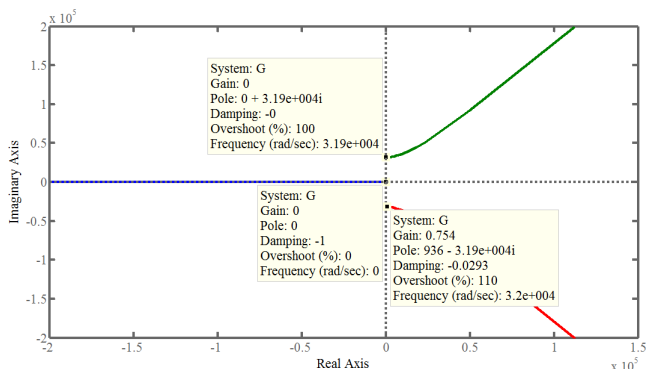


Figure 4. Root locus diagram of open-loop system G(s).

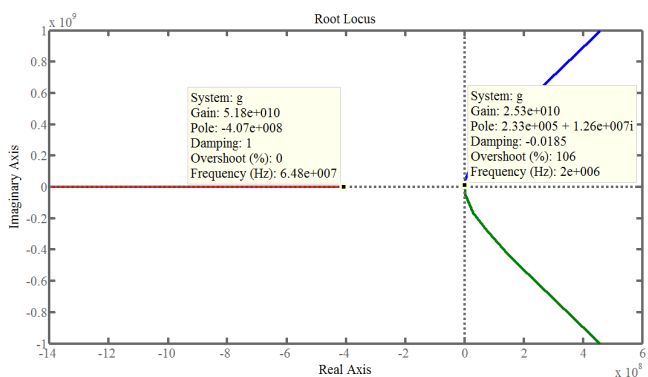


Figure 5. Root locus diagram of the closed-loop system $G_1(s)$.

From Figure 5, it is clear that the overshoot of our closed-loop system is less as compared to the open-loop systems and also that the bandwidth of the system has been increased due to the inclusion of the controller within the loop. Also, the damping has increased so the settling time of the system has decreased implying that the system has become more stable.

4. Proportional Controller

4.1 Effect of Inner-loop Gain K_c on System Performance

The inner-loop gain K_c is varied and the resulting plots are recorded for a proportional controller (Figures 6,7), while the proportional gain K_p is kept constant at a value of 1.63. The reference tracking capabilities are increasing as the value of inner-loop gain K_c is increased from 0 - 1.4. From 1.6 - 3, we are getting the best possible results and

onward from 3, the THD in the output signal is increased although it still maintains good reference tracking. The THD injected into the system at PCC is 2.494%. For inner-loop gain $K_c = 0$ our system is unstable. For inner-loop gain $K_c = 1.4$ the system is stable but after 0.04 seconds, it starts getting unstable and THD in the signal is increasing. From Table 1, at inner-loop gain K_c equal to 1.6 we have reached our optimal performance as far as reference tracking is concerned.

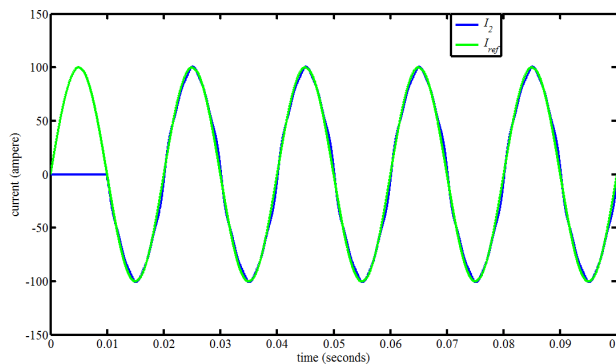


Figure 6. Plot of $I(t)$ vs t , inner-loop gain $K_c = 3$.

At the value of inner-loop gain K_c equal to 3, we are getting the optimal phase margins and the gains margins along with a reduced value of THD. Figure 8, shows the bode plot of output current with respect to the reference current for the best controller gain at which the gain margins and phase margins are optimal. The results of our findings have been mentioned in Table 1.

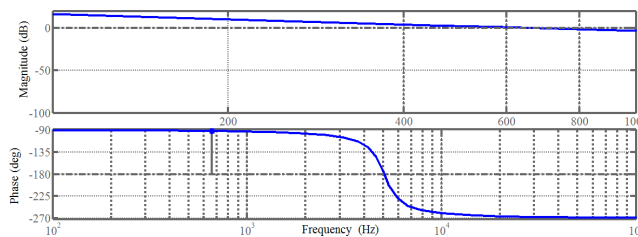


Figure 7. Bode plot of I_2 w.r.t. I_{ref} for optimal gain i.e., inner-loop gain $K_c=3$.

Table 1. Effect of variation of inner-loop gain k_c on system performance

S. No	K_c	THD	G.M (dB)	P.M ($^\circ$)	Stable
1	0	3804	undefined	-90	No
2	1.4	64.93	-0.161	-5.96	No
3	1.6	4.512	0.998	88.9	Yes
4	3	4.544	6.46	88	Yes
5	20	5.815	22.9	77	Yes

5. Proportional Integral Controller

This is basically the implementation of the Table 2 given in the paper⁸. We are varying the value of proportional gain K_p and integral gains K_I taking the inner-loop gain $K_c = 3$. With the increase in the value of the proportional gains K_p and integral gains K_I beyond the value of 1, the gain margins and phase margins are diminishing. The best performance of the controller is found at the value of 1.65. The bode diagram is shown in Figure 9.

Table 2. Effect of variation of proportional K_p and integral K_I gains on thd

S.No	K_p	K_I	Gain Margin	Phase Margin (°)	THD	Stable
1	1	1	10.7	88.8	2.965	Yes
2	2	2	4.68	87.4	6.027	Yes
3	3	3	1.16	85.9	29.65	Yes
4	3.4	4	0.0726	1.92	45.81	Yes
5	3.5	4	-0.179	-3.9	18150	No
6	2.8	2.8	1.76	86.2	16.95	Yes
7	1.65	1.65	6.35	87.9	4.606	Yes

For proportional gain $K_p =$ integral gain $K_I = 1$, the output is under-damped and I_2 is over-exceeding the value of the reference current. The value of THD is less so the disturbance rejection is good. For proportional gain $K_p =$ integral gain $K_I = 2$, the output signal is over-damped and the THD has increased. For proportional gain $K_p =$ integral gain $K_I = 3$, the controller is able to follow the reference for the first cycle, but when a higher order disturbance enters the system at the beginning of the second cycle, the controller totally fails. For proportional gain $K_p = 3.4$, integral gain $K_I = 3$, we have reached the upper limit for the gains and should work within this range rather than trying to go beyond.

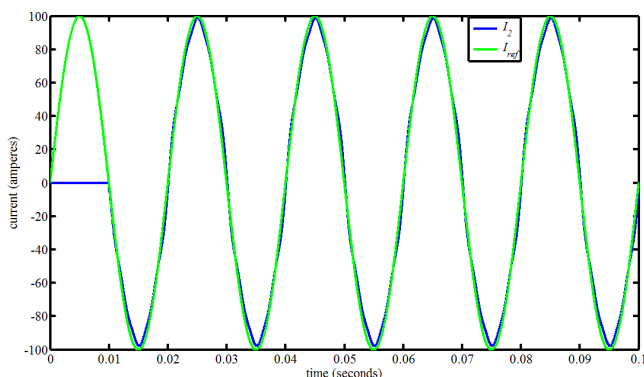


Figure 8. Output current w.r.t reference current for optimal gains.

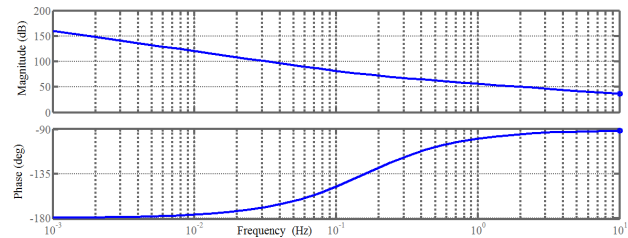


Figure 9. Bode plot showing the response of I_2 w.r.t I_{ref} for the optimal gains $K_p = K_I = 1.65$.

6. Conclusion and Future Work Include THD Output using FFT Analysis

We can use the proportional and proportional integral controllers to give the desired performance under utility THD below 5% for certain gains. But even in the range of gains that has been explored in this text, the controller performance is limited. PI controller is not a very good controller in the sense that it is not very effective at tracking a high frequency reference signal. The frequencies of our system and the controller to be used should be given special importance when choosing a particular controller and also its bandwidth.

We can control the d-q currents rather than the output current and compare their performances to establish which is more effective. The Repetitive Controller (RC) can be used to control the current either in simulation or by using a DSP based hardware platform. Also the study of RC by varying the grid frequency is also an interesting prospect for future work. The practical application of this model is in a Photo-Voltaic (PV) panels and in wind turbines which are connected to the grid through a suitable converter.

7. References

1. Sharkh SM, Abusara MA, Orfanoudakis GI, Hussain B. Power Electronic Converters for Microgrids. New Jersey, USA: John Wiley and Sons Ltd; 2014 Apr. ISBN 978-0-470-82403-0.
2. Jamil M, Hussain B, Sharkh SM, Abusara MA, Boltryk R J. Microgrid Power Electronic Converters: State of The Art and Future Challenges. Proceedings of the IEEE 44th International Universities Power Engineering Conference (UPEC); 2009 Sep 1–4; Glasgow: Southampton, United Kingdom: IEEE. p. 1–5.
3. IEEE Standard for Interconnecting Distributed Resources with Electric Power Systems; IEEE Std 1547. 2003. p. 1–28.
4. Jamil M, Sharkh SM, Abusara MA, Boltryk RJ. Robust Repetitive Controller Feedback Control of a Three-Phase Grid

- Connected Inverter. IET 5th International Conference on Power Electronics and Drives; 2010 Apr 19–2; United Kingdom: IET. p. 1–66.
5. Jamil M, et al. Design and Analysis of Odd-Harmonic Repetitive Control for Three-Phase Grid Connected Voltage Source Inverter. *Review on Electrical Engineering (Przeład Electrotechniczny)*; 2013. 1a: 292–95. ISSN: 00332097.
 6. Abusara MA, Jamil M, Sharkh SM. Repetitive Current Controller for Interleaved Grid-Connected Inverters. *IEEE 3rd International Symposium on Power Electronics for Distribution Generation Systems (PEDG)*; 2012 Jun 25–28; Aalborg: IEEE. p. 558–63.
 7. Jamil M. Repetitive Current Control of Two-Level and Interleaved Three-Phase PWM Utility Connected Inverters [PhD Thesis]. United Kingdom: Faculty of Engineering and the Environment, University of Southampton; 2012 Feb.
 8. Haseeb M, Jamil M, Faisal M, Firdousi F. Analysis of Three-Phase Two-Level PWM Inverter with LCL Filter using Classical Controllers for Renewable Energy Sources. *Proceedings of International Conference on Energy and Sustainability*; 2013 Apr 27; Karachi, Pakistan: NED UET. p. 63–67.
 9. IEEE Recommended practice for utility Interface of Photovoltaic Systems (PV); IEEE Std 929-2000.
 10. Liserre M, Blaabjerg F, Hansen S. Design and Control of an LCL Filter based Three-Phase Active Rectifier. *IEEE Transactions on Industry Applications*. 2005; 41(5):1281–91.
 11. Jamil M, Sharkh SM, Abusara MA. Current Regulation of Three-Phase Grid Connected Voltage Source Inverter Using Robust Digital Repetitive Control. *International Review of Automatic Control (Theory and Applications)*; 2011 Mar. 4(2):211.
 12. Jamil M, et al. DSP Based Hardware Implementation of Repetitive Current Controller for Interleaved Grid Connected Inverter. *Review on Electrical Engineering (Przeład Electrotechniczny)*; 2013. 2a: 251–55. ISSN: 00332097.
 13. Jamil M, Arshad R, Rashid U, Ayaz Y. Design and Analysis of Repetitive Controllers for Grid Connected Inverter Considering Plant Bandwidth for Interfacing Renewable Energy Sources. *Proceedings of 2014 IEEE International Conference on Renewable Energy Research and Applications (ICRERA)*; 2014 Oct; Milwaukee, USA: IEEE. p. 19–22.